Reader's Companion

Chapters 1–3: The Physical Properties of Fluids, Kinematics of the Flow Field, Equations Governing the Motion of a Fluid

Chapters 1, 2 and 3 deal with the physical, kinematical and dynamical aspects of fluids, respectively. Actual fluid mechanical phenomena are only considered from Chapter 4 onward, where a restriction is made to the laminar motion of an incompressible homogeneous fluid. The results quoted in the first three chapters are not restricted to any particular sub-field of fluid dynamics, and thereby, have a general validity. While the focus here is on the fundamentals, there are nevertheless a few aspects that deserve mention.

Sections 1.6–1.8 in Chapter 1 include an insightful discussion of the similarities and differences between gases and liquids, and the underlying transport mechanisms at the molecular level in each case. Section 2.3 in Chapter 2 has a detailed analysis of the kinematics of local relative motion[2]. In Chapter 3, the Newtonian approximation to the deviatoric stress tensor is obtained in Section 3.3 by using the isotropy of the fluid microstructure. Interestingly enough, the author remains unconvinced about the alternate argument that appeals to the absence of a deviatoric stress in solid-body rotation. In Section 3.4, a definitive discussion of the equilibrium in a moving fluid is given, and emphasis is placed on the density and the internal energy, both of which retain an unambiguous interpretation in the absence of exact thermodynamic equilibrium. Next is a discussion of the rather subtle departure from equilibrium in an isotropic flow

[2] A footnote on page 88 of the book already points out the crucial difference between accelerating and decelerating flows in the context of blowing out a match!

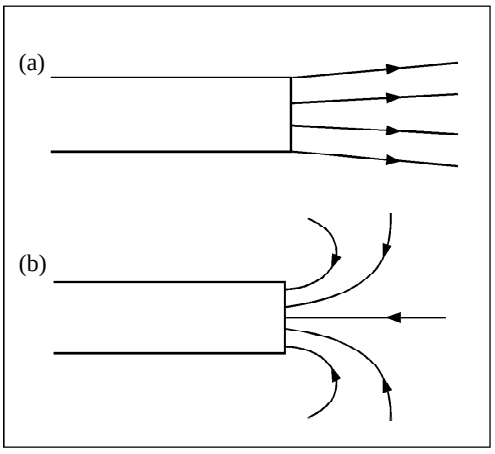

Figure 1. It is easy to put out a match or candle by blowing on it, but it is almost impossible to blow out a candle or a match by sucking. This is because the flow coming out of a tube or orifice and that entering it are very different. The flow leaving a tube is like a jet with the velocity decaying slowly with distance. The flow entering the tube comes from all around, and is hardly 'felt' a short distance away. This is the reason we do not breathe in the same air that we breathe out! Working of a putt-putt boat is based on this phenomenon. (See V Sharada and Jaywant H Arakeri, Resonance, Vol. 9, Nos. 6 and 7, 2004.)

field. Although, an expression for the resulting non-equilibrium normal stress (expressed as a bulk viscosity times the rate of deformation) is derived using a phenomenological approach, care is taken to point out the underlying molecular mechanism; that the difference between the thermodynamic and mechanical pressures arises due to the existence of internal degrees of freedom other than translational ones, and the lack of an exact equipartition of energy between the various degrees of freedom in presence of an imposed deformation. Under conditions where vibrational degrees of freedom contribute significantly to the internal energy, the Newtonian approximation breaks down, and the history of the motion has to be taken into account via a Maxwell-like constitutive relation (see Lighthill [6]). In Section 3.5, the Bernoulli's theorem is presented in a number of specialized limits, and further, it is shown that for one-dimensional steady flow, the Bernoulli constant is conserved even for a viscous conducting fluid. The chapter concludes with a careful discussion of the conditions under which the fluid velocity field may be regarded as solenoidal. Compressibility effects become important in three different scenarios – when fluid velocities become comparable to the sound speed (the familiar Mach number constraint in gas dynamics), when the flow time-scale is of the same order as that of sound waves with wavelength comparable to a characteristic flow length scale (as in acoustics), or if the size of the domain becomes large enough for the change in static pressure on account of body forces to be comparable to the absolute pressure (a limit of relevance to meteorology, the relevant length scale then being the scale-height of the atmosphere).

Glossary

Vorticity: Vorticity (= curl of velocity vector) in fluid flow is related to 'net' rotation of fluid elements; fluid elements translate, rotate and deform, whereas rigid bodies only translate and rotate.

Vortices: Vortices are often seen as long tubes with the fluid moving in circular paths around the local axis of the tube.

Irrotational or potential flow: When vorticity is zero, we have potential flow. The governing differential equations for potential flow are linear and instantaneous, and greatly simplify the analysis. In high Reynolds number flows, large regions of the flow domain, away from boundary layers, are often irrotaional.

Reynolds number (Re): (= density * velocity scale * length scale/dynamic viscosity) is a measure of the ratio of inertia forces to viscous forces. At very low Re (low velocity, small length scale or high viscosity), pressure and viscous forces are roughly in balance; for example, pollen grain falling in air, or a body moving in a very viscous liquid. At high Re, the balance is between pressure and inertia forces, except in boundary layers where viscous effects are always important . Prandtl showed that however low the viscosity, its effect may never be neglected.

Points Worth Noting

The author gives an alternate form of the Navier–Stokes equation with the divergence of the viscous stresses being expressed as a curl of the vorticity field. The relation is purely a result of kinematics, but a specific consequence is that a potential flow field continues to be an exact solution of the Navier–Stokes equations. Thus, the general failure of irrotational flow theory is not because irrotational flow fields do not satisfy the Navier–Stokes equations, but rather due to an inability of these fields to satisfy the no-slip boundary condition imposed by viscosity.

The author relates the incompressibility constraint to the ratio of the change in the pressure associated with a moving fluid element, relative to the absolute pressure. Various forces effecting such a change, including inertial acceleration and body forces, naturally lead to the different circumstances under which changes in the density of a fluid element may be regarded as negligible.

Chapter 4: Flow of a Uniform Incompressible Viscous Fluid

Section 4.1 discusses the circumstances under which a modified pressure may be used in the equations of motion, particularly, an interpretation in terms of an Archimedian buoyancy even in the presence of rotation with Coriolis and centrifugal forces. Section 4.2 considers steady unidirectional flow, and the author comes up with an ingenious application for the viscous flow through a pipe of rectangular cross-section – the thickness of a layer left on a wall by a moving paint brush! Section 4.3 adds time dependence, and examples include the viscous diffusion of a sheet vortex and unsteady pipe flow evolving under the imposition of a uniform axial pressure gradient.

Section 4.4 examines Ekman transport in a rotating fluid, in particular, the fluid motion induced in a semi-infinite domain by an applied stress. Owing to Coriolis forces, the fluid motion describes a spiral, starting at an angle of 45^{o} to the applied stress, and moving further away with increasing depth. The net flux of fluid is at right angles to the applied stress. The problem applies to the mechanics of wind-generated ocean currents, provided the actual kinematic viscosity is replaced by an effective momentum diffusivity that models the transport of momentum due to turbulent velocity fluctuations in the oceans. Section 4.5 describes both steady and unsteady flows with circular streamlines, including the steady flow between concentric rotating cylinders and the self-similar evolution of an initially localized axisymmetric distribution of vorticity (the Lamb–Oseen vortex).

Section 4.6 considers an exact solution of the Navier–Stokes equations: the steady axisymmetric jet due to a point source of momentum. In appropriate limits, the solution reduces to the velocity

field of a real laminar jet with an imposed momentum flux and the flow induced by a translating particle in the absence of inertia. The next section discusses the principle of dynamical similarity, and the status of the Reynolds number (Re) as the single most important dimensionless parameter governing the motion of an incompressible homogeneous fluid. Section 4.8 considers flows with negligible inertia including lubrication flows, flow through a porous medium and in a Hele-Shaw cell. In the latter instance, the depth-averaged velocity field is, in fact, irrotational which, rather paradoxically, makes the cell a useful device to visualize potential flow fields. Next, the minimum dissipation theorem is used to demonstrate the uniqueness of a solution to the inertialess equations of motion (Re = 0). A useful application of this theorem is to show that a particulate suspension must have a shear-thickening bulk rheology in presence of inertia (see Ryskin [7]).

Section 4.9 examines particle motion at small Re. The inertialess flow field due to a translating solid sphere is derived and leads to the Stokes drag. In Section 4.10, the author emphasizes the singular nature of the Stokes approximation. The inertial terms become important at large distances (beyond a so-called inertial screening length), and reflect the inability of a small sphere to drag an infinite body of fluid along with it. The equations governing the velocity field, on length scales of the order of the inertial screening length, were first put forth by Oseen. The Oseen solution is fore-aft asymmetric, and at large distances, has the character of a source field everywhere except in a narrow wake which provides the compensating inflow. This structure of the far-field velocity disturbance is generic and, as shown in Section 5.12, applies to a translating body at any Re. Section 4.11 analyzes problems relevant to the calculation of effective transport coefficients in multi-phase systems. The shear viscosity of a dilute emulsion is obtained from the response of an isolated drop to an linear flow; for large disperse phase viscosities, it reduces to the viscosity of a dilute suspension first derived by Einstein (see Leal [8]). Next, the effective bulk viscosity of a dilute bubbly dispersion is determined via a calculation of the dissipation rate (due to the shear viscosity!) associated with the disturbance velocity field of a single bubble.

The concluding section analyzes the flow field around a translating bluff body as a function of Re. Besides the canonical instance of a circular cylinder (and the Kármán street that results beyond a critical Re), the author also discusses a translating sphere, where the asymmetry of the vortex shedding process is noted. Recent research has shown that the axisymmetric wake in this case indeed undergoes a bifurcation to a plane-symmetric configuration at a critical Re, and a second bifurcation thereafter leads to the unsteady scenario (see Natarajan and Acrivos [9] and Jenny *et al* [10]). See *Figures* 2 and 3.

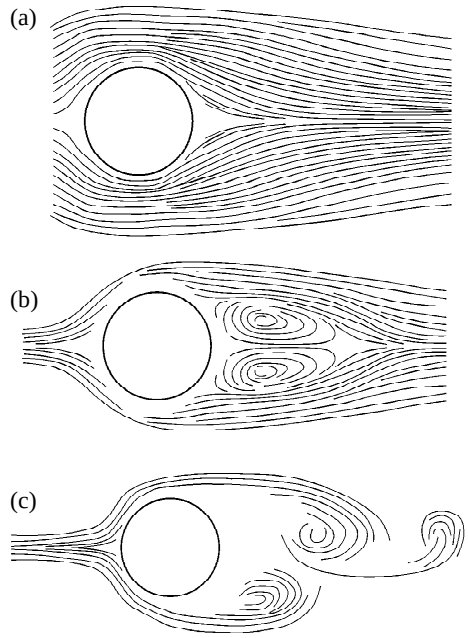

Figure 2. The figures show flow past a circular cylinder at three different Reynolds numbers. a) At low Re (=10), the flow is attached and nearly fore-aft symmetric. As Re increases the flow detaches or separates. b) Re = 25: Two closed eddies form at the rear of the cylinder. c) Re = 2000: The flow is fully separated and a Bénard–Kármán vortex street is formed further downstream. Separation is responsible for the high drag on bluff (non-streamlined) bodies. Asymmetric separation leads to swing in cricket balls. (See Jaywant H Arakeri and P N Shankar, Resonance, Vol. 5, No. 12, pp.48–63, 2000; Raghuraman N Govardhan and O N Ramesh, Vol. 10, No. 8, pp. 25–37, 2008).

Figure 3. The beautiful Bénard–Kármán vortex street formed by a cylinder at Re = 100. Vortices are shed alternately, giving rise to an oscillatory side force that can lead to failure of tall structures like chimneys.

Points Worth Noting

The author mentions the difficulty of accounting for the emergence of steady re-circulating eddies at the rear of a translating bluff body, since the notion of boundary layer separation is a rather tenuous one at the modest values of Re concerned. The explanation offered is a mere imbalance between the amount of vorticity generated and that which can be convected away downstream so as to maintain the no-slip condition without the need for a back flow. The explanation gains further credence for a translating bubble with a free-surface boundary layer (analyzed in Chapter 5), where a recirculating wake is seen as a strictly finite Re phenomenon; for instance, it appears behind an oblate bubble (of a fixed eccentricity) at a finite Re only to disappear as Re $\rightarrow \infty$ when the entire flow field approaches the corresponding potential flow solution (see Leal [11]).

The author extends the analysis for a translating solid particle to a drop. Even in the Stokes regime, however, the drop translation problem is a more difficult one, since the drop shape is unknown apriori. It is shown that the normal stress balance at the drop interface is identically satisfied for a spherical shape. Thus, rather surprisingly, provided the Reynolds number is small, a drop remains spherical regardless of the relative magnitudes of the (deforming) viscous and (restoring) interfacial tension forces; in dimensionless terms, the drop shape is independent of the Capillary number in the Stokes regime. This is attributed as the reason why even relatively large air bubbles rising in a very viscous medium like treacle continue to be spherical.

Chapter 5: Flow at Large Reynolds Number: Effects of Viscosity

In Section 5.1, the author emphasizes the importance of the no-slip condition, one that is entirely responsible (via separation) for the divergence between the actual flow field at large Re and that predicted from inviscid theory. Section 5.2 deals with vorticity dynamics. The vorticity equation is interpreted as the rate of change of angular momentum of an instantaneously spherical fluid element in response to viscous stresses. The physical significance of the vortex-stretching term is emphasized, and vorticity intensification via stretching, made possible at high Re, is noted. (For further details on the mechanics of vorticity in both inertial and non-inertial frames, see Lighthill [12, 13]). The latter is typical of turbulent flows, and a simple example, the Burgers vortex, exemplifies the generation of steep vorticity gradients via a balance of strong uni-axial stretching and viscous diffusion; similar to a turbulent flow field, the dissipation rate per unit length in a Burgers vortex is independent of viscosity. In Section 5.3, it is argued that vorticity in a homogeneous fluid is largely produced by the action of viscosity at rigid boundaries, and that the mechanisms evolving it are strictly local since pressure forces do not exert a direct influence. Thus, the vorticity field at large Re tends to be compact (in space), allowing for an economical description of the fluid dynamics. A discussion of Kelvin's circulation theorem follows where the author also emphasizes the baroclinic mechanism in a heterogeneous fluid as a source of vorticity, and the ability of a multi-valued potential, such as that due to electromagnetic forces, in generating circulation.

Section 5.4 contains a detailed explanation of how viscous forces, via the no-slip condition, act as a source of vorticity. In general, the vorticity evolution may be regarded as occurring in three stages – the initial generation of an irrotational flow field with a vortex sheet at the rigid boundary, rapid diffusive broadening of the vortex sheet, and finally, a balance of convection and diffusion that sets up the steady-state vorticity distribution when it exists. The author draws an analogy between the vorticity and temperature fields while noting the incompleteness of the analogy since, aside from boundary conditions, the vorticity field is constrained to be the curl of the velocity field that convects it. Section 5.5 illustrates typical vorticity distributions set up

from a balance of convective and diffusive fluxes. Examples include the stagnation point flow near a rigid boundary and the centrifugal flow due to a rotating disk. The former offers possibly the simplest illustration of a displacement thickness.

Section 5.6 examines Jeffery–Hamel flow in two dimensions, one of the few non-trivial exact solutions of the Navier–Stokes equations (see Rosenhead [14]). The problem illustrates the crucial difference between accelerating and decelerating flows in presence of rigid boundaries. In the former instance (a converging channel), the flow tends to the intuitive form expected at large Re, viz., that of an inviscid irrotational plug at the centre together with asymptotically thin vortical layers along the inclined walls. For a diverging flow, however, there exist regions of flow reversal throughout the domain[3]. Although the structure becomes finer in scale with increase in Re, effects of viscosity remain significant in all parts of the domain even as $\mathrm{Re} \to \infty$; this serves as a counter-example to the boundary layer hypothesis introduced in the next section.

Section 5.7 discusses the concept of a boundary layer and the leading-order parabolized equations are obtained via standard scaling arguments. Section 5.8 examines the laminar boundary layer on a flat plate, and the resulting $O(\mathrm{Re}^{-1/2})$ drag coefficient. While the solution of the boundary layer equations is standard, the author also indicates the manner in which one might obtain higher-order corrections. For instance, a better approximation to the outer flow is obtained by calculating the irrotational flow around a virtual boundary determined by the boundary layer displacement thickness. The resulting tangential velocity distribution at the boundary may then be used to obtain an improved approximation for the flow within the boundary layer. This would lead to a correction of $O(\mathrm{Re}^{-1})$ to the drag coefficient for a flat plate. As it turns out, the actual correction is slightly larger, being $O(\mathrm{Re}^{-7/8})$, and arises from a region of $O(\mathrm{Re}^{-3/8})$ localized near the trailing edge. The triple deck theory framework leading to this result was developed just after the publication of Batchelor's text (see Stewartson [15][4], Messiter [16], Schlichting [17]).

Section 5.9 analyzes the effects of acceleration in the external flow. As in Section 5.6, the boundary layer is found to be extremely sensitive to mild decelerations. Separation is thus

[3] There exist multiple solutions even for the converging case for large enough Re. However, any flow reversal in this case is restricted to the asymptotically thin boundary layers.

[4] In attempting to analyze the flow near the trailing edge and the resulting correction to the drag on the plate, Stewartson, in an earlier paper (see Stewartson [18]), erroneously concluded that the modification to the Blasius boundary layer was restricted to a region of $O(\mathrm{Re}^{-3/4})$ where the governing equations were the full Navier–Stokes equations; a year later, the correct analysis that accounted for displacement thickness effects in a larger region of $O(\mathrm{Re}^{-3/8})$ was in place.

inevitable in the rear of a blunt object, and an analysis for short times, of flow past a cylinder, shows that the time for the onset of backflow is inversely proportional to the peak deceleration. Boundary layer separation is considered in more detail in Section 5.10. Both the cases of a smooth deceleration and those of a sudden deceleration, as in flow past a body with a salient edge, are analyzed. The latter instance is simpler in that the location of separation is fixed by the salient edge, and the resulting separation acts to eliminate the original region of deceleration. As shown in Section 6.7, this is the idea underlying the development of a circulation around an aerofoil; the initial separation acts to move the rear stagnation point towards the trailing edge of the aerofoil. Section 5.12 offers a unified treatment of wakes, jets and free shear layers using the boundary layer concepts developed in Section 5.8, while also pointing out the limitations of the laminar solutions in the context of real, possibly turbulent, jets and wakes.

Section 5.11 examines the force on a body moving in an otherwise quiescent fluid, in particular, the relative magnitudes of the skin and form drag contributions. The latter, for a streamlined body, is of the same dynamical order as the skin drag, and its smallness is due to geometrical reasons. The form drag is indeed an extremely sensitive function of geometry, and increases sharply for a bluff body owing to separation. In juxtaposing the disparate dimensions of a slender aerofoil and a circular cylinder experiencing the same drag, *Figure* 5.11.2 provides a dramatic illustration of this geometry dependence, thereby highlighting the importance of streamlining. The author goes on to note the well-known reduction in drag when Re exceeds a certain large critical value ($\sim 10^5$), a fact related to a laminar-turbulent transition in the attached boundary layer; as a matter of detail, the author attributes the decrease in drag to a transition in the detached (rather than attached) boundary layer. The laminar-turbulent transition in boundary layers around bluff bodies, and lateral forces that result from any asymmetry, are a crucial component to understanding the dynamics of swing and spin in sports including cricket and tennis (for instance, see Kundu and Cohen [19]).

Section 5.13 analyzes oscillatory boundary layers. The energy dissipation approach is first used to characterize the linearized damped oscillations of a rigid particle. Next is an analysis of the steady streaming induced by non-linear stresses in the oscillatory boundary layer; this is of relevance to the secondary vortical flows induced by the irrotational flow field associated with stationary acoustic modes. Section 5.14 examines the boundary layer on a free surface. The latter also acts as a source of vorticity. However, the vorticity generated is proportional to the interface curvature, and for a fixed shape of the interface, remains $O(1)$ even as $\mathrm{Re} \to \infty$. As the author points out, the deceleration of the external stream is weak and separation is unlikely unless the curvature becomes large. Separation in flow past sufficiently large bubbles occurs for precisely this reason, however. Numerical computations show the presence of recirculating eddies behind sufficiently oblate bubbles (see Ryskin and Leal [20]). An extreme instance of

such a flow occurs for spherical-cap bubbles (see Section 6.11) where the recirculating wake transitions to a turbulent state. In the absence of separation, the potential flow field provides a uniformly valid approximation for the velocity field in the entire domain including the boundary layer. Another consequence of the reduced vorticity in a free-surface boundary layer is that the dominant dissipation of mechanical energy occurs in the outer irrotational flow domain. This allows for a remarkably simple calculation of the rise velocity of a spherical bubble at large Re.

Section 5.15 illustrates the value of an integral formulation (or control volume analysis) of the equations of motion. Such macroscopic balance methods are often deceptively simple, yielding valuable information provided care is exercised in the choice of the control volume. The author considers a couple of non-trivial cases. The first one is the flow past a regular array of bodies wherein the drag exerted by the array is found to be the difference between the upstream and downstream pressures; there is an obvious connection here to the permeability of a porous medium. The second example deals with the pressure drop across a sudden expansion, where one may obtain, in a simple way, an expression for the net pressure drop without delving into any details of the viscosity-induced separation.

Points Worth Noting

When discussing the stages involved in the evolution of a vorticity field under the action of viscous forces, the author points to an interesting exception to the general scenario. This occurs for a circular cylinder rotating in an otherwise quiescent fluid. In this case, the vorticity generated at the cylinder surface eventually diffuses out to infinity, leaving behind an irrotational flow field! Thus, the resulting steady velocity field is, on one hand, a solution of the Stokes equations in two dimensions, being known as the 'rotlet', and on the other hand, is also the potential field induced by a point vortex (and thereby, is an exact solution of the Navier–Stokes equations at any Re).

The author notes how the instability of the bluff body wake at finite Re acts to obscure a possibly fundamental connection between the theoretical steady (but unstable) solution to the Navier-Stokes equations in the limit $\mathrm{Re} \to \infty$, and the solutions of the Euler equations with singular stream-surfaces known from free streamline theory. Such a connection has been explored both experimentally and theoretically (see Acrivos *et al* [21, 22, 23], Fornberg [24]).

Chapter 6: Irrotational Flow Theory and its Applications

This chapter presents a discussion of irrotational motion and its applications. As noted at the beginning, the reader is continually reminded of the underlying effects of viscosity, and the crucial role of separation in determining the nature of the potential flow field for large Re.

Section 6.2 develops the fundamentals of irrotational flow theory (the underlying mathematical framework is already developed to an extent in Chapter 2). Among other results, it is shown that a maximum in speed and a minimum in pressure cannot occur at an interior point in the fluid domain; interior stagnation points are allowed, however. Bernoulli's theorem is developed in its familiar form in Section 6.3, and is first used to determine the outflow from a circular orifice in an open vessel. The problem of determining the exit speed is a standard one; but, the author further discusses use of the integral formulation of the equations of motion to determine the diameter of the exit jet that results for different orifice geometries. A modified form of Bernoulli's theorem in a rotating reference frame is developed, and then used to illustrate the principle underlying the action of a centrifugal pump as well as a water sprinkler. Section 6.4 develops the concept of added mass, and its relation to the impulse and kinetic energy of fluid motion. The crucial difference between the nature of potential flow solutions in singly and multiply connected domains is emphasized. In the latter case, the existence of a unique velocity field requires the added specification of a cyclic constant, this being related to the vorticity 'embedded' within the body. The d'Alembert's paradox, and the necessity for a non-zero circulation in order to generate a lift force, is demonstrated. The acceleration reaction acting on a body moving unsteadily in an ambient time-dependent flow is obtained. Section 6.5 discusses the complex potential for irrotational flow in two-dimensions, particularly, the use of conformal mapping to determine the flow field in and around complex domains. Section 6.10 provides a physical interpretation of the velocity potential, which may be thought of as the pressure impulse needed to set up a given irrotational motion from rest.

Section 6.6 discusses the flow past a circular cylinder with circulation. For small values of the circulation, the flow field itself appears to have little relevance due to the strong deceleration in the aft-region that would invariably lead to separation. The expression for the lift is nevertheless central to aerofoil theory, and it is shown in Section 6.7 that an identical lift acts on a slender aerofoil. Herein, the author considers the flow past an impulsively started inclined flat plate (a model for the aerofoil). Although there is a rapid deceleration towards the rear stagnation point in the initial irrotational flow field, the ensuing separation and the shedding of a starting vortex provides the attached viscous boundary layer with the circulation necessary for the generation of a lift. Viscosity, in effect, makes the rear stagnation point coincide with the trailing edge, removing the original potential flow singularity. The value of the resulting circulation may thus be calculated within the inviscid framework. The author proceeds with an economical analysis of the lift on a Joukowski aerofoil. It is also worth noting that in the circular cylinder problem, for large values of the circulation, a region of closed streamlines surrounds the cylinder. The absence of a sustained deceleration along the cylinder surface implies that such a flow field may be realized even in a viscous fluid for an appropriate angular velocity.

Section 6.8 discusses irrotational flow in three dimensions, pointing out, to begin with, the absence of an analog of the method of complex variables. The solution for a translating sphere is used to obtain the response of a bubble in an unsteady ambient field. The acoustic characteristics of dilute bubbly dispersions (bubble clouds) is crucially dependent on the dynamic response of a single bubble in an oscillating velocity (pressure) field. Another application is the secondary Bjerknes force that arises between two bubbles undergoing volumetric oscillations in an ambient pressure field, and eventually leads to their coalescence. The degassing of a liquid using ultrasonic vibrations operates on this principle. Next, the irrotational flow field induced by a translating spheroid is obtained. The limiting case of the flow induced by a disk models the initial splash resulting from the impact of a blunt object on a free surface.

Section 6.9 outlines the essential elements of inviscid slender body theory, wherein the disturbance field due to a slender body is obtained as a superposition of fundamental singularities[5]. In the simple instance of a slender body aligned with the flow, the disturbance field may be obtained as a superposition of sources placed along the symmetry axis with the source density being locally determined. The two-dimensional scenario of an inclined slender body is more complicated, however, and requires, in addition, a distribution of circulation, with the circulation density satisfying an integral equation.

Section 6.11 considers the motion of gas bubbles in an otherwise quiescent liquid at large Re. With increasing Re, the shape of a rising bubble changes from a sphere to eventually a spherical cap with a flattened rear end. The complicated flow field around such a bubble is highlighted by an unsteady turbulent wake in its rear. The flow near the front stagnation point, however, remains steady and nearly irrotational, however, and Bernoulli's theorem applied to the surface streamline yields a deceptively simple expression for the rise velocity, $U = \alpha\,(ga)^{1/2}$, α being a shape factor related to the interior boundary (bubble + wake) around which the (near) potential flow occurs. The formula also provides an accurate approximation to the rate of rise of the mushroom cloud created by a nuclear explosion, and may be used to estimate the thickness of the draining film that eventually forms on the walls of a vertical tube initially full of liquid. Finally, the Rayleigh–Plesset equation, obtained via a novel energy argument, is used to analyze the expansion of a spherical bubble.

Section 6.12 examines cavitation together with the reasons for its occurrence in liquids; the latter include the presence of high velocities (tip vortices associated with propeller blades) and large negative pressures (liquids subject to large-amplitude acoustic pulses). The Rayleigh–

[5] The author also wrote what is arguably the most influential article on viscous slender body theory (see Batchelor [25]).

Plesset equation provides an estimate for the enormous pressures attained in collapsing cavities, highlighting their potential for damage. If the thermodynamics of phase change is unimportant, the distinction between vapor and gas-filled cavities is lost, and the flow field, in the absence of gravity, is characterized by Re and the cavitation number (K); the latter is a function of the cavity pressure relative to a suitable reference. For a steady inviscid cavity, the flow field and cavity shape are functions of K alone, and their determination comes under the purview of free streamline theory. This application of the theory is more realistic than the originally intended one (as a model for bluff body wakes for $\mathrm{Re} \to \infty$) since potential flow provides a reasonable approximation for the flow past free surface of the cavity. Section 6.13 applies the theory to determine the flow field and drag for a flat plate oriented broadside-on with an attached cavity at ambient pressure in its rear. This is followed by a qualitative discussion of the theoretical and experimentally observed cavity shapes as a function of K.

Points Worth Noting

A rising bubble is one of the few situations where potential flow theory, as applied to a translating sphere, continues to provide a uniformly valid representation of the velocity field in the entire domain in the limit $\mathrm{Re} \to \infty$. The latter limit is only a theoretical one, since as mentioned above, with increasing Re, the inertial forces also become strong enough to flatten the bubble. There nevertheless remains an accessible intermediate range of Re, where the bubble is approximately spherical, and a potential flow calculation leads to an accurate estimation of the drag coefficient.

In the context of a rising spherical cap bubble, it is worth noting that the rise velocity is obtained without the need to consider the mechanism of the retarding force that balances buoyancy. The author takes it to imply that the magnitude of the retarding force, and the associated dissipation of mechanical energy, must be independent of viscosity; in turn, implying that turbulent stresses must control the transport of momentum in the bubble wake.

Chapter 7: Flow of Effectively Inviscid Fluid with Vorticity

The chapter presents a comprehensive discussion of inviscid rotational flows. Section 7.1 begins with the Biot–Savart law, and a brief discussion of the dynamics of the vorticity field in two-dimensional and axisymmetric flows. Vorticity associated with a material element is conserved in two dimensions, while it is the ratio of the vorticity to the transverse distance from the axis of symmetry that is conserved in axisymmetric flows. The author then shows that the speed with which a thin vortex filament propagates under the action of its own induced velocity field diverges logarithmically with decreasing cross-section. The singularity arises due to the dominant effect of elements of the filament in the neighborhood of a given element (the local

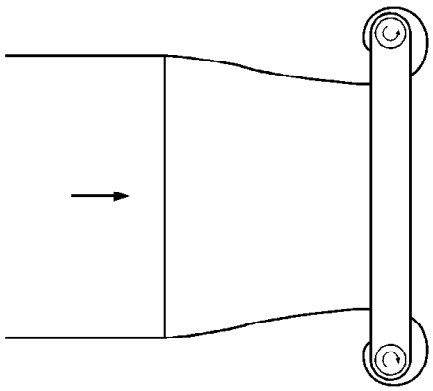

Figure 4. A smoke ring, scientifically termed a vortex ring, is an intriguing entity. A vortex ring is generated by blowing out a puff of fluid from a tube or orifice. Once generated, the toroidal ring travels long distances on account of a self-induced motion.

induction approximation). A consequence is that the speed of a vortex ring grows as the logarithm of its cross-section, and an infinitely thin vortex ring must propagate infinitely fast. The result is counter-intuitive, particularly if one's intuition is based on the two-dimensional analog of a pair of counter-rotating point vortices. Taylor [26], in a short paper, related the parameters of the irrotational flow, induced by an impulsively started circular disk in an ideal fluid, to those of the thin-cored vortex ring that would result from the roll-up of the vortex sheet that remains on dissolution of the disk; later experiments involving the generation of vortex rings, and the theoretical interpretations of the process, rely precisely on such a matching principle (see Gharib, Rambod and Shariff [27], Linden and Turner [28]). The analysis in Section 7.1 also highlights the degenerate nature of the two-dimensional scenario involving interacting point vortices (a popular model with an attractive Hamiltonian structure); in particular, the singular nature of the any three-dimensional perturbation must always be kept in mind.

Next is a discussion of the Kelvin– Helmholtz instability of a vortex sheet. The mechanism is beautifully illustrated in *Figure* 7.1.3. Differential convection of vorticity in the deformed vortex sheet leads to a periodic accumulation, and the resulting induced velocity field reinforces the original deformation. The Kelvin–Helmholtz mechanism operates even for a smooth vorticity distribution provided the wavelength of the sheet deformation is larger than the characteristic transverse scale of the vorticity distribution. With the incorporation of a density difference and a surface tension, the analysis applies to the generation of waves at the free surface of a liquid.

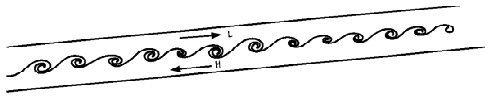

Figure 5. Kelvin–Helmoltz instability occurs when there is 'shear' in a flow. This instability is beautifully and simply illustrated by having a long tube with one-half filled with a heavy liquid, and the other half with a lighter liquid. The tube is initially horizontal and the interface between the two liquids is also horizontal. Tilting the tube slightly will cause the heavy liquid (H) to slide down, and the lighter liquid (L) to slide up. The resulting shear causes the interface to roll-up into vortices.

Section 7.2 discusses the dynamical invariants associated with an inviscid rotational flow. The concept of a distributed impulse is introduced. The first few moments of the impulse lend themselves to a physical interpretation, and relate to the total impulse, the moment of impulse and kinetic energy of the fluid motion. In applying these concepts to vortex rings, the author conjectures the existence of a one-parameter family of rings bounded at one extreme by a torus of an infinitesimal cross-section, and at the other, by the well-known Hill's spherical vortex. The members of such a family were later constructed and analyzed by Fraenkel, [29] and Norbury [30], and have come to be known as the Fraenkel–Norbury family.

Section 7.3 deals with two dimensional flows. The vorticity being conserved along a streamline, the streamfunction ψ satisfies $\nabla^2 \psi = -f(\psi)$, f being an arbitrary function of ψ that may be related to upstream conditions. Exact solutions arising from particular forms of $f(\psi)$ are given. One of the examples is the motion of a slightly deformed circular vortex patch. Infinitesimal amplitude wavy deformations, the 2*D*-Kelvin modes, travel along the edge of the patch at a characteristic speed. A nice argument illustrates how these modes may be treated as vortex sheets at the edge of the patch, and the resulting dynamics implies that they always lag the motion in the vortical core. A familiar finite amplitude analog of these 2*D*-Kelvin modes is the Kirchhoff vortex (see Saffman [31]).

Section 7.4 examines the lift on bodies in inviscid rotational flows, an appropriate generalization of two-dimensional aerofoil theory. The lift has two contributions: the usual one associated with vorticity embedded in the attached boundary layer, and an additional one proportional to the ambient vorticity. The author notes the inherent limitation of the inviscid rotational scenario in that there is no flux of vorticity across streamlines. Viscous effects may thus play a crucial role over long times in regions of closed streamlines. This forms the essence of the Prandtl–Batchelor theorem (see Batchelor [32]) which states that the vorticity in two-dimensional closed streamline regions must eventually be uniformly distributed, while that in steady axisymmetric flow must be proportional to the distance from the symmetry axis.

Section 7.5 considers inviscid axisymmetric flow with swirl. A swirling flow is particularly sensitive to an imposed axial deceleration, a behavior reminiscent of conventional viscous boundary layers. A mild deceleration arises naturally in aircraft trailing vortices on account of viscosity (see Batchelor [33]). For a vortex tube embedded in an external irrotational flow, there arises the peculiar situation wherein no downstream cylindrical state exists beyond a critical deceleration[6]. The connection of this anomaly with the vortex-breakdown phenomenon is

[6] A closer examination suggests that the problem is not the lack of a downstream state. The governing transcendental relation allows, in principle, for an infinite number of states corresponding to a given deceleration, as characterized by a Rossby number (Ro). Thus, the lack of existence must be interpreted as a discontinuous jump of the solution from one branch to another beyond a critical Ro^{-1}.

mentioned. An alternate explanation of the phenomenon also finds mention, an elegant one proposed by Benjamin [34, 35] that treats the breakdown as a non-linear transition between conjugate states, the downstream state being sub-critical and capable of sustaining axisymmetric standing waves (the underlying idea thus being similar to a shock wave or a hydraulic jump); for more recent work on this remarkable phenomenon, see Leibovich [36], Escudier [37] and Rusak and Wang [38]). There also exist regions of parameter space where there is a downstream flow reversal. The author comments on the difficulty in interpreting these solutions, within the framework described, owing to information needed about vorticity arriving from stations further downstream. Finally, there exist critical values Ro for which the downstream velocity profile is singular, and these are interpreted as resonant conditions when the assumption of longitudinal invariance downstream no longer holds and must be replaced by an axisymmetric wave-motion.

Section 7.6 analyzes the axisymmetric oscillations in a rotating fluid. The alternate expansion and contraction of a material curve in a plane transverse to the rotation axis, under the action of the Coriolis forces, is lucidly explained, and naturally leads one to expect wave-like motions in a rotating fluid. (An alternate physical interpretation in terms of the periodic twisting and untwisting of vortex lines is already implicit in Section 7.5). The argument highlights the difference between the nature of Coriolis forces in two and three dimensions. The peculiarity of the swirling state is emphasized. For instance, axisymmetric oscillations in an unbounded domain lack a dispersion relation, and only in the presence of a cylindrical boundary may one sensibly regard the frequency as a function of the wavenumber. In contrast to surface gravity waves, for a given wavenumber, there exist a denumerable infinity of oscillations each with a characteristic radial structure. Further, the swirling base-state does not restrict the amplitude of oscillatory motion. The resulting dispersion curves are robust, and vorticity profiles other than the trivial uniform distribution have dispersion curves of a similar character even in presence of viscosity. Non-axisymmetric oscillations are more complicated, however, due to the selective action of viscosity in a critical layer (see Fabre *et al* [39]). A discussion of plane inertial waves follows. The imposed frequency dictates the direction of energy propagation in these cases, and there exists an exact analogy, in the absence of viscosity, between the characteristics of such waves and those of internal waves in a stratified fluid. (Striking flow patterns arising from such directional energy propagation appear in Greenspan [40] and Turner [41]). The author proceeds to discuss the motion of a sphere along the axis of a rotating fluid as a function of Ro. The Ro = 0 limit is first analyzed when the Taylor–Proudman theorem holds and the motion is two-dimensional. Thus, the sphere pushes along a column of fluid (the Taylor column) spanning the entire domain in the absence of viscosity. This remarkable phenomenon, captured in experiments, is depicted in *Figures* 7.6.2 and 7.6.3. With increasing Ro, the rising sphere sets up inertial oscillations in its wake. The apparently simple problem of a sphere rising in a rotating

liquid for small but finite Ro and large Re is, in fact, one of formidable complexity owing to the complex structure of the viscous Ekman layers that bridge the flow within the column with that outside.

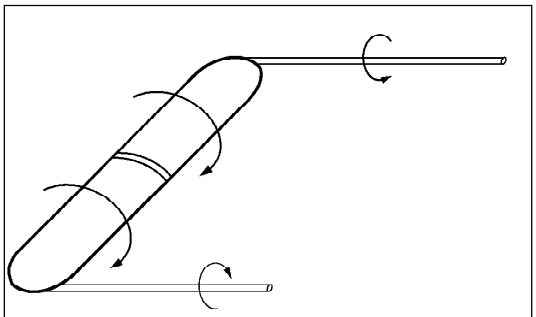

Figure 6. The wing of an airplane or bird experiences a lift arising from a vortex embedded within the wing. This vortex comes out at either end of the wing as a pair of trailing vortices. The energy lost in these vortices accounts for an additional lift-dependent drag called induced drag. The trailing vortices are often seen as two white streaks, the white colour coming from condensed water vapour in the cores of the vortices. (See Jaywant H Arakeri, Resonance, Vol. 14, No. 1, pp.32–46, 2009.)

Section 7.7 discusses the effects of rotation on fluid motion in a thin layer on a sphere. The analysis is carried out in an incompressible shallow-water approximation, but includes the effects of bottom topography, and is thus of relevance to meteorological and oceanographic applications. The topics covered include geostrophic flow and planetary Rossby waves. The chapter concludes with Section 7.8 which discusses the vortex system for a wing of finite span and the resulting induced drag (see *Figure* 6). This is a generalization of the theory for two-dimensional aerofoils in Chapter 6. The discussion includes a brief description of lifting line theory, and hints at the construction of a formal asymptotic theory for lifting wings of finite span with the lifting line analysis providing the leading-order approximation. The final section discusses the modifications that arise for highly swept (delta) wings where the spanwise variation may not be neglected even at leading order. The interesting possibility of a solution with conical symmetry, wherein the distribution of vorticity, in a plane transverse to the wing, remains self-similar, is highlighted.

Points Worth Noting

The mechanism of the Kelvin–Helmholtz instability makes obvious the requirement of an inflection point in the base-state velocity profile for an inviscid instability. An instablity only results from a peak in vorticity, and this added constraint is precisely the generalization of the inflection-point theorem proven by Fjortoft (see Drazin and Reid [42]).

Again, in the context of the Kelvin–Helmholtz instability, the author notes the existence of a second stable root. He relates this to an initial condition engineered in a manner that the mechanisms of convection and accumulation (that would otherwise lead to instability) now lead to a decay of the deformation amplitude. The mathematical reason for the appearance of

complex conjugate roots in inviscid stability analyses is rooted in the time-reversible nature of the Euler equations.

In the context of determining the lift on bodies in inviscid rotational flows, there arises the natural question of extending the analysis to three dimensions. The direction of the lift remains the same; however, the analysis is rendered more difficult since the disturbance field due to the translating particle is no longer irrotational. For a sphere translating in a simple shear flow, the deformation of the ambient vortex lines leads to the generation of streamwise vorticity in its rear (see Lighthill [43] and Auton [44]), and there is an added contribution to the force (mechanistically similar to an induced drag).

The author relates the independent oscillatory motion in fluid planes transverse to the axis of the rotating fluid (induced by Coriolis forces) to the more familiar oscillations of a straight row of suspended bobs endowed with initial transverse displacements that happen to have a particular phase relation. The former corresponds to a plane wave propagating along the axis of rotation, and the analogy immediately implies that such a wave must have a zero group velocity!

Suggested Reading

[1] H Lamb, *Hydrodynamics*, 6th edition, Cambridge University Press, 1932.
[2] L M Milne-Thomson, *Theoretical hydrodynamics*, 5th edition, Dover, 1967.
[3] M Van Dyke, *An album of fluid motion*, Stanford, Parabolic Press, 1982.
[4] L D Landau and E M Lifschitz, *Fluid mechanics*, 2th edition, Pergamon, 1987.
[5] L Prandtl and O G Tietjens, *Applied hydro- and aeromechanics*, McGraw-Hill, 1934.
[6] M J Lighthill, Viscosity effects in sound waves of finite amplitude', *Surveys in Mechanics*, eds: G K Batchelor, and R M Davies, Cambridge University Press, 1956.
[7] G Ryskin, The extensional viscosity of a dilute suspension of spherical particles at intermediate microscale Reynolds numbers, *J. Fluid Mech*., Vol.99, pp.513–529, 1980.
[8] L G Leal, *Laminar flow and convective transport processes*, Butterworth–Heinemann, 1992.
[9] R Natarajan and A Acrivos, The instability of the steady flow past spheres and disks, *J. Fluid Mech*., Vol.254, pp.323–344, 1993.
[10] M Jenny J Dusek and G Bouchet, Instabilities and transition of a sphere falling or ascending freely in a Newtonian fluid, *J. Fluid Mech*., Vol.508, pp.201–239, 2004.
[11] L G Leal, Vorticity transport and wake structure for bluff bodies at finite Reynolds number, *Phys. Fluids*, A1(1), pp.124–130, 1989.
[12] M J Lighthill, Introduction. Boundary layer theory, in *Laminar boundary layers*, Ed. L Rosenhead, pp.46–109, 1963.
[13] M J Lighthill, Dynamics of rotating fluids: a survey, *J. Fluid Mech*., Vol.26, pp.411–431, 1966.
[14] L Rosenhead, The Steady Two-Dimensional Radial Flow of Viscous Fluid between Two Inclined Plane Walls, *Proc. Roy. Soc. A*, Vol.175, pp.436–467, 1940.
[15] K Stewartson, On the flow near the trailing edge of a flat plate, II., *Mathematika*, Vol.16, pp.106–121, 1969.
[16] A F Messiter, Boundary layer flow near the trailing edge of a flat plate, *SIAM J. Appl. Math*., Vol.18, pp.241–257, 1970.
[17] H Schlichting and K Gersten, *Boundary layer theory*, Springer, 2001.
[18] K Stewartson, On the flow near the trailing edge of a flat plate, *Proc Roy Soc Long*, Vol.A306, pp.275–290, 1968.
[19] P K Kundu and I M Cohen, *Fluid mechanics*, Academic Press, 1990.

[20] G Ryskin and L G Leal, Buoyancy-driven motion of a gas bubble through a quiescent liquid, *J. Fluid Mech*., Vol.148, pp.19–35, 1984.
[21] A S Grove, F H Shair, E E Petersen and A Acrivos, An experimental investigation of the steady separated flow past a circular cylinder, *J. Fluid Mech*., Vol.19, pp.60-86, 1964.
[22] A Acrivos, D D Snowden, A S Grove and E E Petersen, The steady separated flow past a circular cylinder at large Reynolds numbers, *J. Fluid Mech*., Vol.21, pp.737–760, 1965.
[23] A Acrivos, L G Leal, D D Snowden and F Pan, Further experiments on steady separated flows past bluff objects, *J. Fluid Mech*., Vol.34, pp.25–48.
[24] B Fornberg, A numerical study of steady viscous flow past a circular cylinder, *J. Fluid Mech*., Vol.98, pp.819–855, 1980.
[25] G K Batchelor, Slender-body theory for particles of arbitrary cross-section in Stokes flow, *J. Fluid Mech*., Vol. 44, pp.419–440, 1970.
[26] G L Taylor, Formation of a vortex ring by giving an impulse to a circular disk and then dissolving it away, *J. Appl. Phys*, Vol.24, p.104, 1953.
[27] M Gharib E Rambod and K Shariff, A universal time scale for vortex ring formation, *J. Fluid Mech*., Vol.360, pp.121–140, 1998.
[28] P F Linden and J S Turner, The formation of 'optimal' vortex rings, and the efficiency of propulsion devices, *J. Fluid Mech*., Vol.427, pp.61–72.
[29] L E Fraenkel, Examples of steady vortex rings of small cross-section in an ideal fluid, *J. Fluid Mech*., Vol. 51, pp.119–135, 1972.
[30] J Norbury, A family of steady vortex rings, *J. Fluid Mech*., Vol.57, pp.417–431, 1973.
[31] P G Saffman, *Vortex dynamics*, Cambridge University Press, 1992.
[32] G K Batchelor, The lift force on a spherical body in a rotational flow, *J. Fluid Mech*., Vol.1, pp.177–190, 1956.
[33] G K Batchelor, Axial flow in trailing line vortices, *J. Fluid Mech*., Vol.20, pp.645–658, 1964.
[34] T B Benjamin, Theory of the vortex breakdown phenomenon, *J. Fluid Mech*., Vol.14, pp.593–629, 1962.
[35] T B Benjamin, Some developments in the theory of vortex breakdown, *J. Fluid Mech*., Vol. 28, pp.65–84, 1967.
[36] S Leibovich, Vortex stability and breakdown: Survey and extension, *AIAA J*., Vol.22, pp.1192–1206, 1984.
[37] M Escudier, Vortex breakdown: observations and explanations, *Prog. Aerospace Sci*., Vol.25, pp.189–229, 1988.
[38] Z Rusak and S L Wang, Review of theoretical approaches to the vortex breakdown phenomenon, *AIAA Paper*, pp.96–2126, 1996.
[39] D Fabre, D Sipp and L Jacquin, The Kelvin waves and the singular modes of the Lamb-Oseen vortex, *J. Fluid Mech*., Vol.551, pp.235–274, 2006.
[40] H Greenspan, *The theory of rotating fluids*, Cambridge University Press, 1968.
[41] J S Turner, Buoyancy effects in fluids, Cambridge University Press, 1973.
[42] P G Drazin and H Reid, *Hydrodynamic stability*, Cambridge University Press, 1981.
[43] M J Lighthill, 1953, Drift, *J. Fluid Mech*., Vol.1, pp.31–53.
[44] T R Auton, The lift force on a spherical body in a rotational flow, *J. Fluid Mech.*, Vol.183, pp.199–218, 1987.

Ganesh Subramanian is a faculty fellow at the Engineering Mechanics Unit in JNCASR, Jakkur, Bangalore 560 064, India. His research interests span a range of phenomena in complex fluids and flows. These include the dynamics and rheology of complex fluids such as suspensions, emulsions, polymer solutions and granular gases, the collective dynamics of active particle suspensions, hydrodynamic stability of multi-phase flows, vortex dynamics, and the origin of the Ramdas layer.

Email: sganesh@jncasr.ac.in